

Proceeding Paper

Design and In Silico Evaluation of Some Non-Nucleoside MbtA Inhibitors (Pyrazoline Based Mycobactin Analogs) as Anti-Tubercular Agents: On Track to Tackle Tuberculosis [†]

Gourav Rakshit and Venkatesan Jayaprakash *

Department of Pharmaceutical Sciences and Technology, Birla Institute of Technology, Mesra, Ranchi 835215, Jharkhand, India; gouravr16@gmail.com

* Correspondence: drvenkatesanj@gmail.com

† Presented at the 26th International Electronic Conference on Synthetic Organic Chemistry; Available online: <https://ecsoc-26.sciforum.net>.

Abstract: The WHO database shows that *Mycobacterium tuberculosis* has become an epidemic worldwide due to its pathogenicity and virulence, which have magnified its infectiousness. The situation becomes grimmer with the prevalence of MDR-TB, XDR-TB, emergence of cross-resistance, ineffectiveness of novel therapeutic targets, failure of novel medications in clinical trials, currently available drugs losing their therapeutic efficacy, lack of drug discovery efforts due to poor ROI, and the existence of co-infections, i.e., HIV, TB, COVID, and HIV-TB-COVID. Following our prior studies described by Stirret et al., 2008, Ferreras et al., 2011, & Shyam et al., 2021 herein we focus on exploring pyrazoline-based mycobactin analogs (non-specific mycobactin biosynthesis inhibitors) targeting MbtA enzyme (1st step of mycobactin biosynthesis) with a hope of finding a more potent analog showing a high affinity for MbtA. Design strategy involves retaining the structural features of mycobacterial siderophores. Herein, we designed a small library (12 molecules) of mycobactin analogs keeping the necessary scaffold (diaryl-substituted pyrazoline (DAP)) intact and assessed their stability using in silico tools. To find the binding modalities and inhibitory profile of the proposed compounds, they were docked in the active site of the MbtA receptor (by analogy with the homologous structure PDB: 1MDB). The lowest energy conformation of each docked ligand (best score) was visualized. All compounds were evaluated for their ADMET (absorption-distribution-metabolism-excretion-toxicity) profile. The best molecule which revealed a good ADMET profile was taken up for MD simulation study (45 ns). Results revealed that the designed compounds **GV08** (−8.80 kcal/mol, 352.58 nM), **GV09** (−8.61 kcal/mol, 499.91 nM), **GV03** (−8.59 kcal/mol, 508.51 nM), and **GV07**, (−8.54 kcal/mol, 553.44 nM) had good docking score and inhibition constant. Of these **GV08** showed a good ADME profile with all major parameters lying in the acceptable ranges. They also showed the least toxicity with no hepatotoxicity and skin sensitization. MD simulation studies of **GV08** also suggest that the protein-ligand complex is stable throughout the simulation as was evidenced by RMSD, RMSF, and H-bond plots. The future scope invalidates these findings through synthesis, characterization, and intracellular activity.

Citation: Rakshit, G.; Jayaprakash, V. Design and In Silico Evaluation of Some Non-Nucleoside MbtA Inhibitors (Pyrazoline Based Mycobactin Analogs) as Anti-Tubercular Agents: On Track to Tackle Tuberculosis. *2022*, *4*, x.

<https://doi.org/10.3390/xxxxx>

Academic Editor(s): Julio A. Seijas

Published: 15 November 2022

Publisher's Note: MDPI stays neutral with regard to jurisdictional claims in published maps and institutional affiliations.



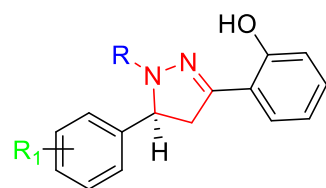
Copyright: © 2022 by the authors. Submitted for possible open access publication under the terms and conditions of the Creative Commons Attribution (CC BY) license (<https://creativecommons.org/licenses/by/4.0/>).

Keywords: antitubercular drug discovery; MbtA; molecular docking; MD simulation; mycobactin; siderophores; pyrazolines; non-nucleoside MbtA inhibitors

1. Introduction

Mycobacterium tuberculosis, the causative agent of tuberculosis, is an airborne, infectious, and ultimately fatal bacillus that causes tuberculosis (Mtb) [1]. This disease has been plaguing humans for centuries and has recently become a major international health concern. To eradicate tuberculosis by 2030 is one of the key health objectives of the United Nations Sustainable Development Goals. The World Health Organization released its

Global Tuberculosis Report on 14 October 2021, providing an in-depth look at the devastating effects of this illness [2]. In 2020, there were 5.8 million new cases of infection reported worldwide, putting us right back where we were in 2012 [3]. Additionally, 1.5 million HIV-negative people died around the world. Reduced access to TB diagnosis and treatment, as well as a lack of drug discovery initiatives, are likely to blame for these concerning infection rates. The increasing prevalence of MDR-TB and XDR-TB, emergence of cross-resistance, the fact that current targets were resistant to treatment, the ineffectiveness of novel therapeutic targets, and the failure of novel medications in clinical trials has prompted the development of novel chemotherapeutic treatments with improved efficacy over the currently available drugs [4]. The gradual appearance of drug-resistant cases to these new drugs portends a bleak future for anti-tubercular chemotherapy. The burden is further increased by the occurrence and emergence of co-infections with HIV, TB, COVID, and HIV-TB-COVID [5]. This emphasizes the necessity employing novel chemical entities functioning through unique mechanisms to combat the growing threat of this infectious killer disease on a worldwide scale. This can be achieved by employing the concept of “conditionally essential target” (CET)-based drug design. The identification and targeting of conditionally essential targets are a common focus in the development of effective chemotherapeutic treatments for infectious diseases (CET). To this end, we are applying a theory proposed by Prof. Luis E. N. Quadri, who hypothesized that concentrating on a conditionally necessary pathway in the host-pathogen machinery would aid in the discovery of new antibacterial drugs. One such CET that has been shown to be useful in the mycobacterial life cycle and replication is the mycobactin biosynthesis pathway (MBP) [6]. In response to iron-deficient conditions, mycobacteria up-regulate the MBP and begin to uptake mycobactins (siderophores/iron chelators). The mycobactin megasynthase cluster encodes a mixed nonribosomal peptide synthetase-polyketide synthase (NRPS-PKS) system that is responsible for the synthesis of mycobactin (siderophore). This cluster consists of 14 conditionally essential genes (mbtA–mbtN). Salicyl-AMP ligase (MbtA) and phenyloxazoline synthase (MbtB) are two essential enzymes in this biosynthetic pathway. For this reason, it has been deemed a potentially fruitful endogenous target for the discovery of novel lead molecules/inhibitors. As a possible MbtA inhibitor, nucleoside analogues have been studied extensively since the turn of the millennium. Our lab at BIT Mesra is focusing on finding non-nucleosidic analogues instead, as these have poor pharmacokinetic profiles. Our objective is to generate non-nucleosidic analogues (pyrazoline-based mycobactin-mimicking compounds) that retain the structural features of mycobacterial siderophores in the hope that they will inhibit the siderophores biosynthesis enzyme (MbtA), thereby stopping bacterial growth in iron-deficient environments. Herein, we investigate MbtA enzyme-targeting pyrazoline-based mycobactin analogues (non-specific mycobactin biosynthesis inhibitors) (1st step of mycobactin biosynthesis). To find a more potent analogue displaying high affinity for MbtA (adenylating enzyme) in the *in silico* exercise, we wish to investigate the structural diversity of the previously found active compounds, as described in our previous studies by Stirret et al. (2008) [7], Ferreras et al. (2011) [8], and Shyam et al. (2021) [9]. In line with these previous researches; our goal was to find novel compounds (non-nucleosidic analogues) having high affinity for MbtA. So, we designed a small library (12 molecules) of mycobactin analogues that retained the diaryl-substituted pyrazoline (DAP) scaffold. The designed molecules along with their structures are presented in Table 1. The putative compounds were docked in the MbtA receptor active site to determine their binding affinities and inhibitory profiles (by analogy with the homologous structure PDB: 1MDB). Top four docked ligand’s lowest energy conformation (highest score) was displayed in BIOVIA discovery studio [10]. The absorption, distribution, metabolism, excretion, and toxicity (ADMET) profile of the top four compounds was analyzed. Good ADMET profile molecules were selected for further MD simulation (45 ns).

Table 1. Tabular representation of the designed molecules.

Sl. No.	Code	R	R ₁
01	GV01		2-CH ₃
02	GV02		3-CH ₃
03	GV03		4-CH ₃
04	GV04		2-OCH ₃
05	GV05		3-OCH ₃
06	GV06		4-OCH ₃
07	GV07		2-Cl
08	GV08		3-Cl
09	GV09		4-Cl
10	GV10		2-OH
11	GV11		3-OH
12	GV12		4-OH

2. Materials and Methods

2.1. Hardware and Software Employed

Docking simulations of current study was done using a DELL workstation running Ubuntu 20.04.3 LTS (64-bit as OS, Intel® Core™ i7-11,800 CPU@2.30 GHz processor, 16 GB RAM, 4 GB GPU), and hard disk drive of 1 TB. Software used was autodock-4.2.6 program for the docking purpose, ChemDraw 19.0 (Perkin-Elmer) for sketching and preparation of ligand. Visualizations were done using UCSF Chimera 1.13.1. [11], BIOVIA Discovery Studio Visualizer program was used for the generation of 2D ligand-protein interaction diagrams. Molecular dynamics simulations (MDSs) were carried out using GROMACS [12,13].

2.2. Docking Simulations

2.2.1. Protein Structure Preparation

The crystal structure of Gene: mbtA consisting of Protein Salicyl-AMP ligase/salicyl-S-ArCP synthetase with UniProt ID: P71716 was selected for the study. The 3D X-ray crystallographic structure/PDB file was obtained from AlphaFold Protein Structure Database [14,15]. The protein.pdb file was opened in Autodock Tools (ADT), the solvent and ions were removed and the resulting structure was saved as a .pdbqt file for use in Autodock 4.2.6 [16].

2.2.2. Ligand Preparation

The designed small molecule ligands were prepared by sketching the 2D structures in ChemDraw 19.1. The 2D representations were converted into 3D structures using Chem3D 19.1 and energy minimized using the integrated MM2 module with default settings. The final stabilized structures were saved in .pdb format for protein-ligand docking.

2.2.3. Protein-Ligand Docking Simulations

The Autodock-4.2.6 program (ADP) was used for all molecular docking studies [16]. The docking algorithm used was the Lamarckian Genetic Algorithm. ADP tools were used to prepare the protein and ligands. The active site was found using UCSF Chimera 1.13.1, and a binding site box (grid box) that was $60 \times 60 \times 60$ in the x, y, and z dimensions was centered on the nucleotide binding pocket (by analogy with the homologous structure PDB Ref: 1MDB). The default values for all other options were used, i.e., the population size was 150 and the number of Genetic Algorithm (GA) runs was 50. The maximum number of evaluations was 2,500,000. The final procedure involved the running of the auto grid and auto dock. Auto grid-4.2 was used for generating map files and Autodock-4.2 was used for running molecular docking of each ligand on respective protein. From the results file (.dlg), the lowest energy conformation of each docked ligand was retrieved. All docking data were evaluated, and visualizations of various structures were done using Autodock-4.2.

2.3. ADME Prediction

The ADME (absorption, distribution, metabolism, and excretion) of the molecule under investigation, which could be employed as a future lead molecule for drug development, is an important factor in predicting its pharmacodynamics. SWISSADME is a web server built and maintained by the Swiss Institute of Bioinformatics' (SIB) molecular modelling group (<https://www.swissadme.ch>, (accessed on)) [17]. Already created structures of ligands/molecules were uploaded individually in the Marvin JS portion of the website <http://swissadme.ch/index.php> (accessed on) to compute ADME parameters. Structures were automatically translated to SMILES format, and the server predicted ADME. The collected results were stored for further investigation.

2.4. Toxicity Prediction

Toxicology prediction is a crucial feature of all compounds. PkCSM is a web server database that allows users to analyze molecules by either sketching them graphically or providing them in SMILES format [18]. The toxicity information on the web server database includes AMES toxicity, maximum tolerated dose, hepatotoxicity, skin sensitivity, and hERG I and II inhibitors. After logging into the website, the SMILES of the top-scoring compounds after docking were searched and submitted, and toxicity was chosen in prediction mode.

2.5. Molecular Dynamics Simulations

Based on docking and pharmacokinetic results, the lowest energy and best-posed complex of molecule GV08 was selected for the simulation study using Groningen Machine for Chemicals Simulations (GROMACS) 2019 package with CHARMM27 all-atom force field [19]. Ligand topology files were generated using SwissParam (website: <https://www.swissparam.ch/>) [20]. The charge of the system was neutralized by the addition of the sodium and chloride ions. The energy minimization of the complex (50,000 steps) was executed using the steepest descent approach (1000 ps). Finally, 45 ns molecular dynamics simulation with periodic boundary conditions was conducted for the respective protein–ligand complex with 4,50,000 steps. The root-mean-square deviation and fluctuation (RMSD/F), intramolecular hydrogen bonds, radius of gyration (ROG) (Rg), and thermodynamic parameters were analyzed using Xmgrace (<http://plasma-gate.weizmann.ac.il/Grace/>).

3. Results

3.1. Docking Simulation Studies

The docking investigation of all the ligands with MbtA protein showed favorable binding energies and inhibition constants. Top score compounds namely **GV08 (−8.80 kcal/mol, 352.58 nM)**, **GV09 (−8.61 kcal/mol, 499.91 nM)**, **GV03 (−8.59 kcal/mol, 508.51 nM)**, and **GV07 (−8.54 kcal/mol, 553.44 nM)** indicated a high affinity for the binding pocket and had high negative binding energies. The binding energies/docking scores and inhibition constants of all molecules are given in Table 2.

Table 2. Details of docking-based parameters of designed compounds in the binding pocket of target MbtA protein.

Sl No.	Code	Dock Score (kcal/mol)	Inhibition Constant
01	GV01	−8.19	996.73 nM
02	GV02	−8.53	563.3 nM
03	GV03	−8.59	508.51 nM
04	GV04	−8.26	878.26 nM
05	GV05	−7.97	1.45 μM
06	GV06	−7.88	1.67 μM
07	GV07	−8.54	553.44 nM
08	GV08	−8.80	352.58 nM
09	GV09	−8.61	499.91 nM
10	GV10	−7.96	1.47 μM
11	GV11	−7.88	1.67 μM
12	GV12	−7.70	2.29 μM

The binding conformations of the top score four compounds in the active site/binding pocket involved H-bond interactions with residues of the interacting protein. The details of the residues involved in bonding with ligands i.e., H-bond interactions residues are given in Table 3 and the docking images are shown in Figures 1–4.

Table 3. Details of top score identified compounds showing H-bond interacting residues in the binding pocket of MbtA.

Sl No.	Ligand Code	H-Bond Residues
1.	GV08	Glu357, Ala356, Thr462, Gly460
2.	GV09	Glu357, Ala356, Thr462, Gly460, Gly214
3.	GV03	Glu357, Ala356, Thr462, Gly460
4.	GV07	Gly330, Thr462, Gly460

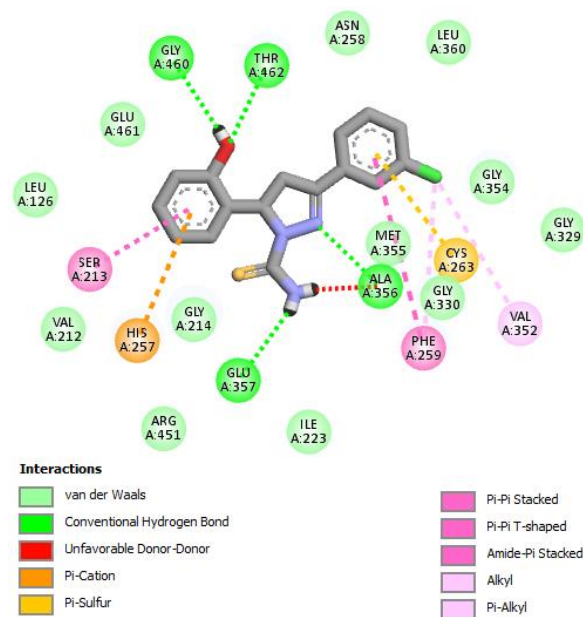


Figure 1. Docking interaction of GV08 in the binding pocket of MbtA showing four hydrogen bonds.

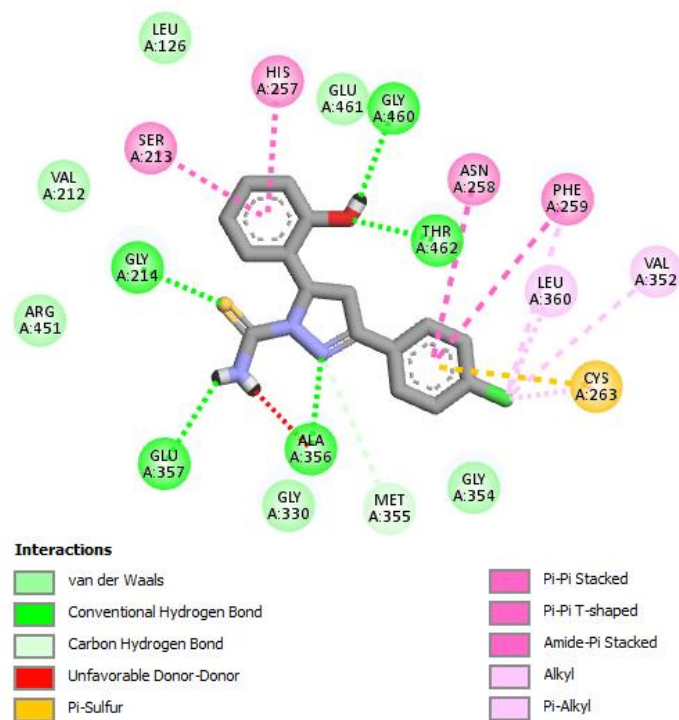


Figure 2. Docking interaction of GV09 in the binding pocket of MbtA showing five hydrogen bonds.

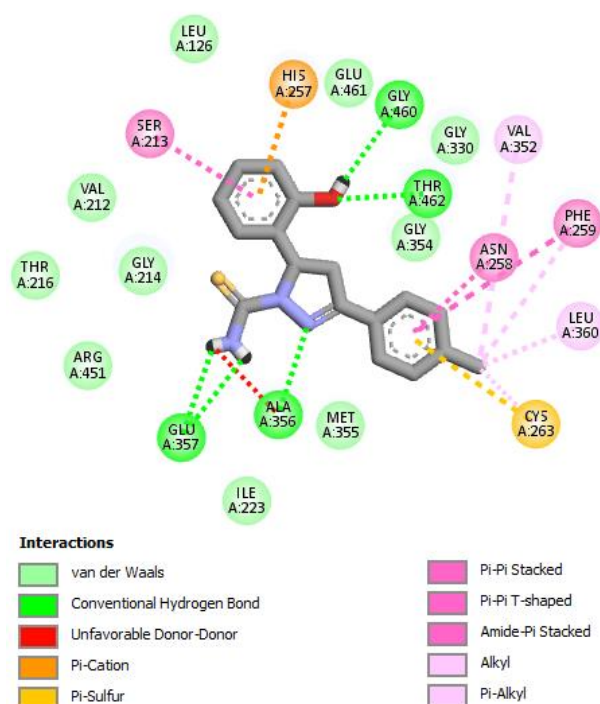


Figure 3. Docking interaction of GV03 in the binding pocket of MbtA showing four hydrogen bonds.

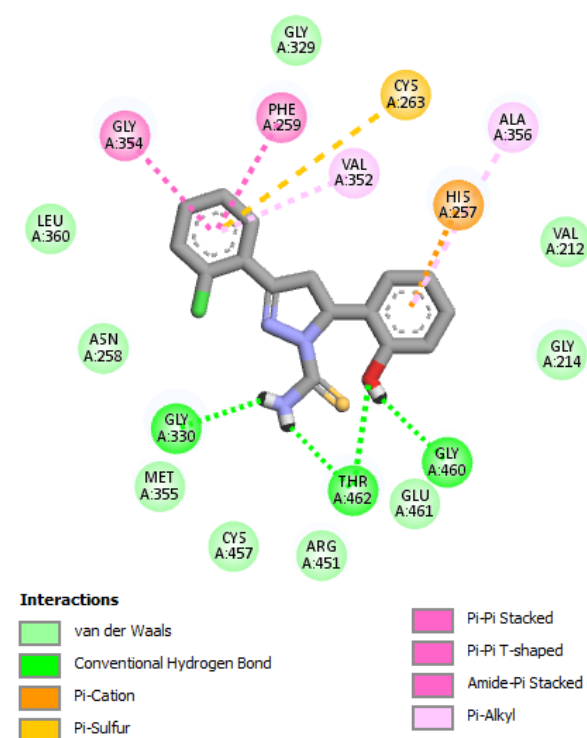


Figure 4. Docking interaction of GV07 in the binding pocket of MbtA showing three hydrogen bonds.

Interaction Analysis of GV08

GV08 revealed a higher binding energy (-8.80 kcal/mol, 352.58 nM). It made four hydrogen bonds with the active site amino acid residues namely: Glu357, Ala356, Thr462, Gly460. Glu357 helps in proton abstraction and donation. The binding of

substrate/inhibitor molecules at the active site induces small movements in the conformation of the protein which is stabilised by the formation of H-bonds. All interactions with amino acid residues help in stabilisation and orientation. The detailed interactions has been presented in Figure 5.

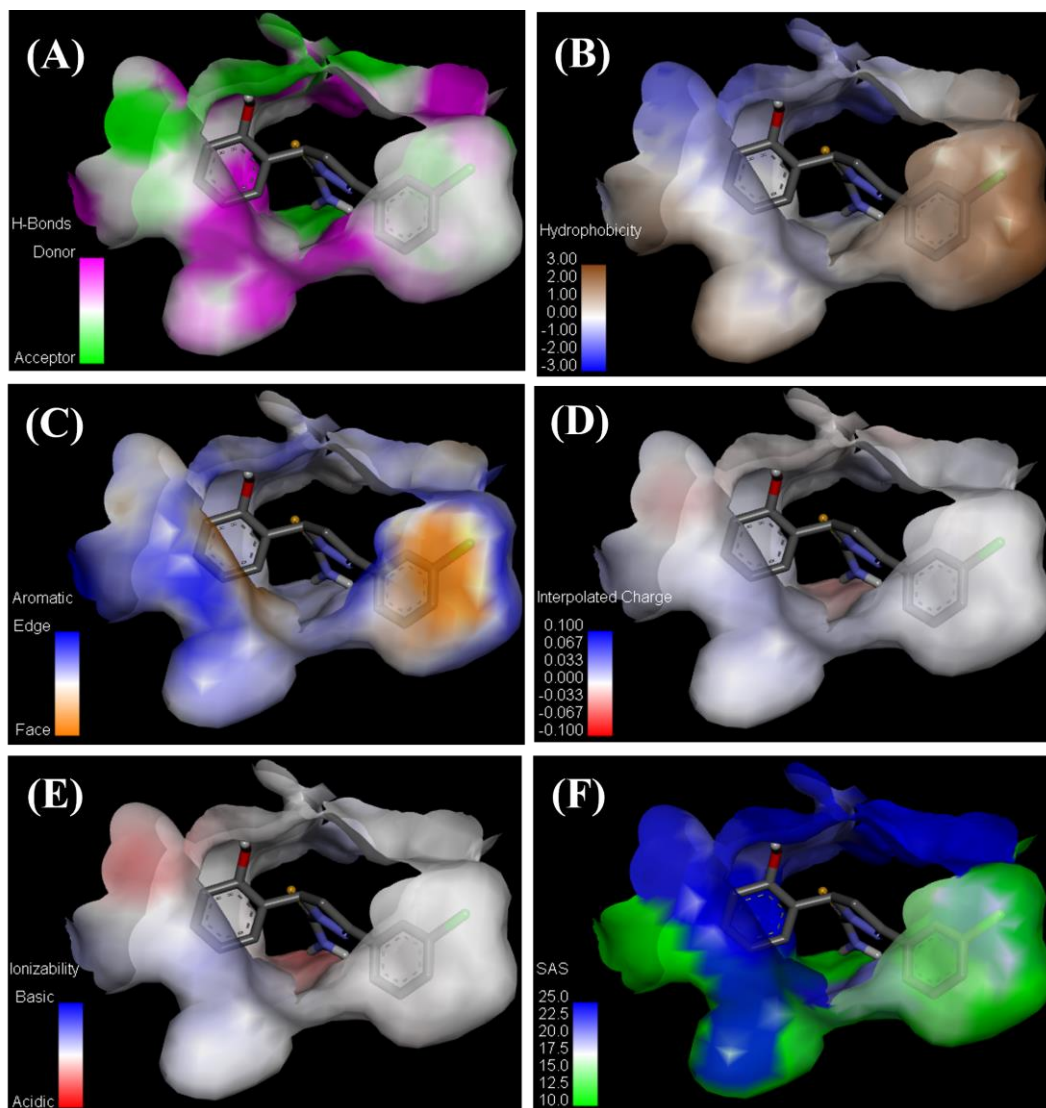


Figure 5. Various interactions of GV08 in the binding pocket of MbtA showing how well the ligand fits in the active site pocket; (A) H-bonds, (B) Hydrophobicity, (C) Aromaticity, (D) Charge distribution, (E) Ionizability, and (F) Solvent accessible surface area.

3.2. ADME Prediction

3.2.1. Results of Drug-Likeness, Bioavailability, Synthetic Feasibility and Alerts for PAINS & Brenk Filters

The likelihood of a compound becoming an oral drug in terms of bioavailability is referred to as drug-likeness. The drug-likeness of our twelve query compounds was calculated using five distinct filters, as shown in Table 4. The results showed that all of the compounds tested (GV08, GV09, GV03, and GV07) had an excellent drug-likeness score and no violations of drug-likeness rules, as well as a good lead-likeness score. To identify the possible uncertain fragments that result in false-positive biological output, the PAINS and Brenk methods were used. As a result of the inclusion of fragments, all compounds were found to be in violation. Along with the synthetic accessibility evaluation, the lead likeness for the compounds was computed. Because their scores were in the range of 3.43–

3.54, the obtained data suggested that these four compounds might be easily synthesised. The Abbot Bioavailability score predicts whether a chemical has 10% oral bioavailability (in rats) or a measurable Caco-2 cell line permeability assay, and is defined by a feasibility value of 11 percent, 17 percent, 56 percent, or 85 percent. All the compounds were predicted at 56 percent, indicating good bioavailability.

Table 4. Tabular representation of different drug-likeness rules, bioavailability, lead-likeness, synthetic accessibility, and alerts for PAINS and Brenk.

SI No.	Compound Code	Drug-Likeness Rules					Alerts		Lead Likeness	Synthetic Accessibility	
		Lipinski (Pfizer)	Ghose (Amgen)	Veber (GSK)	Egan (Pharmacia)	Muege (Bayer)	Bioavailability Score	PAINS			Brenk
1.	GV08	Yes	Yes	Yes	Yes	Yes	0.55	1	1	Yes	3.43
2.	GV09	Yes	Yes	Yes	Yes	Yes	0.55	1	1	Yes	3.43
3.	GV03	Yes	Yes	Yes	Yes	Yes	0.55	1	1	Yes	3.54
4.	GV07	Yes	Yes	Yes	Yes	Yes	0.55	1	1	Yes	3.51

3.2.2. In-Silico Evaluation of Pharmacokinetics Compliance

The success of a drug's trip throughout the body is measured in terms of ADME (absorption, distribution, metabolism, and elimination). By computing the different physico-chemical and bio-pharmaceutical features, the ADME parameters for the substances under research, GV08, GV09, GV03, and GV07, were derived. The molar refractivity, which accounts for the overall polarity of the molecules, was 99.56 (GV08, GV09, and GV07) and 99.51 (GV03) in the acceptable range (30–140). For all compounds, the topological polar surface area (TPSA) was 93.94 Å². These findings indicate that the molecules are unable to pass the blood-brain barrier (BBB). The capacity of a molecule to dissolve itself in a lipophilic medium is referred to as solubility class lipophilicity, and it correlates to various representations of drug properties that affect ADMET, such as permeability, absorption, distribution, metabolism, excretion, solubility, plasma protein binding, and toxicity. The iLOGP and SILICOS-IT results showed that the iLOGP values of the four molecules under investigation (GV08 = 2.43, GV09 = 2.41, GV03 = 2.40, and GV07 = 2.14) were within the acceptable range (−0.4 to +5.6), while the SILICOS-IT values (GV08 = 3.90, GV09 = 3.90, GV03 = 3.77, and GV07 = 3.90) were in the most favourable range. These compounds had a high rate of intestinal absorption. The solubility of a medicine in water is an essential factor in its absorption and distribution. The molecule's solubility in water at 25 °C is represented by log S calculations. The computed log S values through the ESOL model should not exceed 6 for appropriate solubility. The log S value for GV08, GV09, and GV07 was −3.99, whereas the value for GM03 was −3.70, indicating good solubility. The data suggests that these compounds have a good balance of permeability and solubility, and that they would have acceptable bioavailability when given orally. For all compounds, predicted GI absorption was high. Permeability predictions aid in the comprehension of ADMET and cell-based bioassay results. The permeability over human skin for GV08, GV09, and GV07 was −6.19 cm/s, and −6.25 cm/s for GV03, all of which were within acceptable limits. As previously stated, none of these substances demonstrated the ability to penetrate the BBB. Drug-drug interactions and drug bioavailability are sometimes caused by metabolism. Drug-metabolizing enzymes can only bind to the free form of the drug. The interaction of our main compounds with cytochrome P450 enzymes (CYPs), the most well-known class of metabolising enzymes, is critical for understanding their metabolic behaviour. All four compounds were tested for their ability to inhibit CYPs (CYPs of human liver microsomes (HLM)) with minor deviations. Detailed analyses are mentioned in Table 5.

Table 5. Details of in-silico ADME Profile of four selected compounds using Swiss ADME online server.

		GV08	GV09	GV03	GV07	
		C ₁₆ H ₁₄ CIN ₃ OS	C ₁₆ H ₁₄ CIN ₃ OS	C ₁₇ H ₁₇ N ₃ OS	C ₁₆ H ₁₄ CIN ₃ OS	
A D M E T P R O F I L E	Physiochemical parameters	Formula				
		Molecular weight	331.82 g/mol	331.82 g/mol	311.40 g/mol	331.82 g/mol
	Mol. re-fractivity	99.56	99.56	99.51	99.56	
	TPSA	93.94 Å ²	93.94 Å ²	93.94 Å ²	93.94 Å ²	
	Lipophilicity	ILOGP	2.43	2.41	2.40	2.14
		SILICOS-IT	3.90	3.90	3.77	3.90
	Water Solubility	Log S (ESOL), Class	-3.99 Soluble	-3.99 Soluble	-3.70 Soluble	-3.99 Soluble
		Log S (Ali), Class	-4.64 Moderately Soluble	-4.64 Moderately Soluble	-4.37 Moderately Soluble	-4.64 Moderately Soluble
	Pharmacokinetics	SILICOS-IT, Class	-4.69 Moderately Soluble	-4.69 Moderately Soluble	-4.47 Moderately Soluble	-4.69 Moderately Soluble
		GI absorption	High	High	High	High
Pharmacokinetics	BBB permeant	No	No	No	No	
	Log K _p (skin perm.)	-6.19 cm/s	-6.19 cm/s	-6.25 cm/s	-6.19 cm/s	
	CYP1A2	Yes	Yes	No	Yes	
	CYP2C19	Yes	Yes	Yes	Yes	
	CYP2C9	Yes	Yes	Yes	Yes	
	CYP2D6	No	No	No	No	
	CYP3A4	No	No	No	No	

3.3. Toxicity Prediction

The toxicity of the identified compounds **GV08**, **GV09**, **GV03**, and **GV07** was investigated in-silico. The maximum tolerated dosage (human) range for all of the molecules was found to be in between -0.053 and -0.101 Log mg/kg/day. No hERGI and hERG II (human Ether-a-go-go-Related Gene) inhibition was found. The results revealed no intracellular buildup of phospholipids (known to cause QT prolongation, myopathy, hepatotoxicity reaction, nephrotoxicity, and pulmonary dysfunction). The software predicted hepatotoxicity for GV03 only and no cutaneous hypersensitivity in any of the compounds. All the predicted toxicity results of **GV08**, **GV09**, **GV03**, and **GV07** molecules are mentioned in Table 6.

Table 6. Tabular representation data of predicted toxicity of top four compounds.

Model Name	Units	GV08	GV09	GV03	GV07
AMES toxicity	Yes/No	No	No	No	No

Max. tolerated dose (human)	Log mg/kg/day	-0.053	-0.085	-0.101	-0.087
hERG I inhibitor	Yes/No	No	No	No	No
hERG II inhibitor	Yes/No	No	No	No	No
Oral Rat Chronic Toxicity (LD50)	Mol/kg	2.47	2.46	2.393	2.461
Oral Rat Chronic Toxicity	Log mg/kg_bw/day	1.115	1.167	1.313	1.096
Hepatotoxicity	Yes/No	No	No	Yes	No
Skin Sensitisation	Yes/No	No	No	No	No
T. Pyriformis toxicity	Log ug/L	2.113	2.1	2.037	2.127
Minnow toxicity	Log mM	0.629	0.882	1.1	0.893

3.4. Molecular Dynamics Simulations

Molecular dynamics simulation studies were carried out for GV08-MbtA to test the constancy of the ligand binding in the active site of the selected target. MD studies are implemented in many drug discovery applications to study the nature of macromolecules or to interpret mechanisms of drug resistance. The obtained simulation findings are discussed below.

For MbtA protein, the conformations revealed significant RMSD values of 0.45 Å, indicating that the protein–ligand complex was maintained constantly throughout the simulation time. RMSD explains the change in structural confirmations with respect to time. Figure 6, shows the RMSD of protein (0.45 Å) and ligand (7.5 Å).

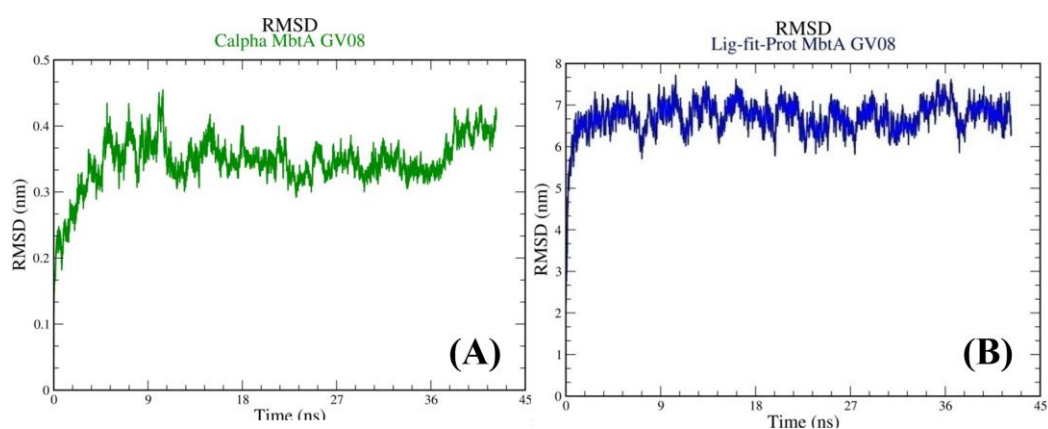


Figure 6. Root mean square deviation (RMSD) of the protein–ligand complex of MbtA with the lowest binding energy compound GV08; (A) RMSD of protein and (B) RMSD of ligand.

The average variation of a particle (such as a protein residue) over time from a reference position is measured by the root-mean-square fluctuation (RMSF) (typically the time-averaged position of the particle). As a result, RMSF examines the structural elements that deviate the most from their mean structure (or least). Herein, the protein fluctuated the least during the course of simulation but there were minor fluctuations in the ligand. These minor fluctuations are acceptable for small biomolecules (Figure 7). These RMSF values suggest the protein–ligand complex’s stability.

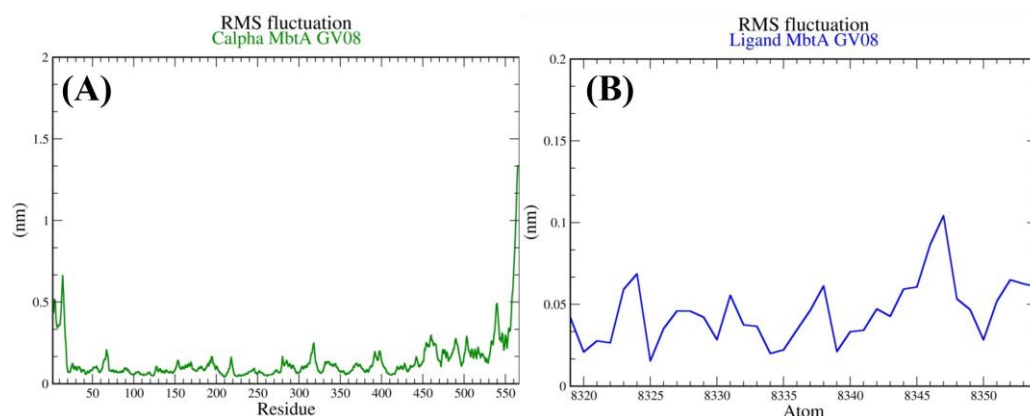


Figure 7. Root mean square fluctuation (RMSF) of the protein–ligand complex of MbtA with the lowest binding energy compound GV08; (A) RMSF of protein and (B) RMSF of ligand.

The stability of the protein–ligand (MbtA-GV08) complex can be justified by various other parameters which suggests the ligand's (GV08) ability to bind to the active site pocket effectively. Figures 8–10 highlights the various parameters associated with the protein–ligand complex during the course of simulation.

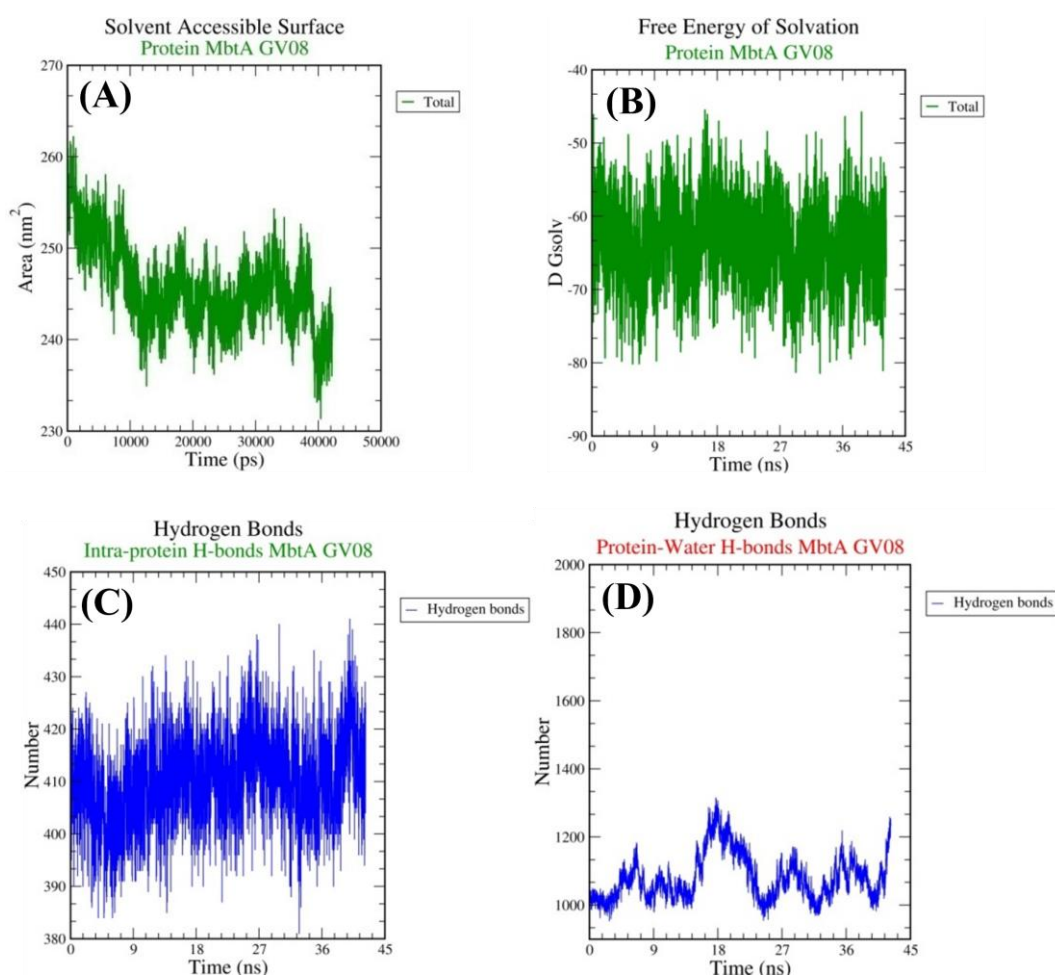


Figure 8. Various parameters of the protein–ligand complex of MbtA with the lowest binding energy compound GV08; (A) Solvent accessible surface area, (B) Free energy of solvation, (C) Intra-protein hydrogen bonding, and (D) Protein-water hydrogen bonding.

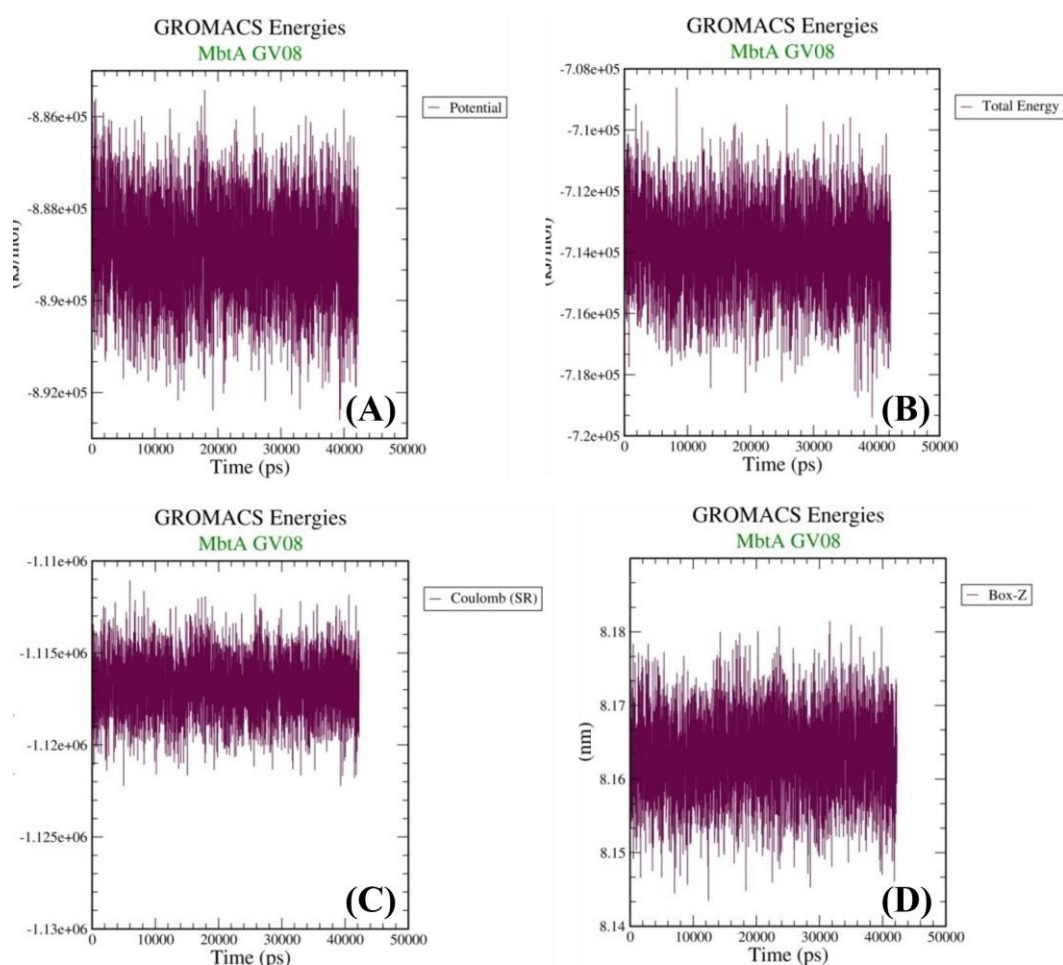


Figure 9. Various thermodynamics parameters of the protein–ligand complex of MbtA with the lowest binding energy compound GV08 highlighting the stability; (A) Potential energy, (B) Total energy, (C) Potential energy, and (D) Density.

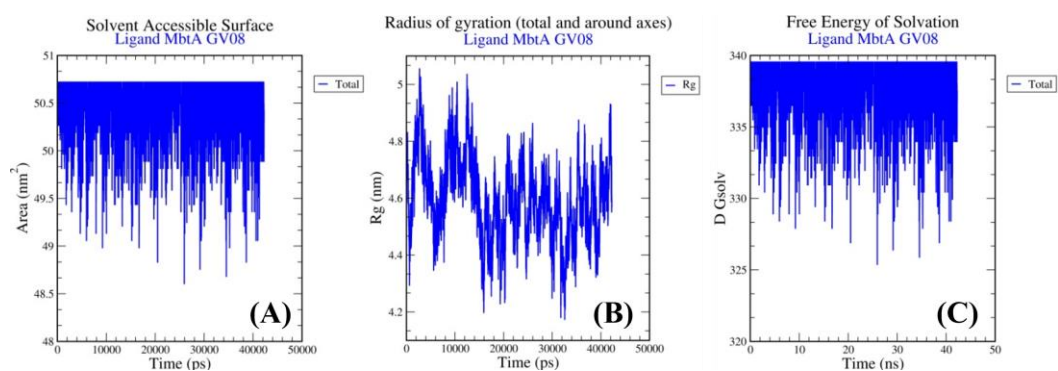


Figure 10. Various thermodynamics parameters of the protein–ligand complex of MbtA with the lowest binding energy compound GV08 highlighting the stability; (A) Potential energy, (B) Total energy, (C) Potential energy, and (D) Density.

4. Conclusion

Despite tremendous advancements in the clinical drug candidate development for TB therapy during the past 10 to 15 years, TB remains a serious health burden in developing countries. Science is still focused on finding treatment possibilities that block novel targets. New treatment targets have been found as a result of research aimed at better understanding the biology of Mtb. It has been proven that imbalances in mycobactin synthesis and iron uptake have a direct impact on mycobacterial virulence and survival in

the host. Structure-based rational design of MbtI and MbtA inhibitors has so far produced intriguing outcomes. In order to do this, we searched for M. tuberculosis inhibitors that can bind to a specific target, namely MbtA, using the concept of CET-based drug design. Our top four identified compounds (GV08, GV09, GV03, and GV07) were found to have strong interactions with the tubercular enzyme MbtA, a newly identified TB target that catalyses the initial two-step process of mycobactin synthesis. Additionally, they displayed a minimal toxicity profile and a decent pharmacokinetic profile. GV08 was found to be the best molecule considering all the above parameters (predicted binding energy and pharmacokinetic profile). The stability of the complex (MbtA-GV08) was evaluated using MD simulation; the results of which revealed good stability. Based on these results it could be concluded that GV08 could serve as a good lead for future optimization. The future scope lies in to validate these findings by performing biological assays. Additionally, looking into the fundamental relationships between possible medications and their therapeutic uses may pave the way for the creation and application of novel and cutting-edge approaches for discovering new antibiotics.

Funding: Gourav Rakshit is thankful to Birla Institute of Technology, Mesra, Ranchi for providing funding in form of Institute Research Fellowship dated March 2021.

Acknowledgments: We would like to express our sincere gratitude to our Department of Pharmaceutical Sciences and Technology, Birla Institute of Technology, Mesra, Ranchi for providing the necessary software and supporting this research work.

Conflicts of Interest: The authors declare no conflict of interest.

References

1. Loddenkemper, R.; Murray, J.F.; Gradmann, C.; Hopewell, P.C.; Kato-Maeda, M. History of tuberculosis. *Tuberculosis* **2018**, *8*–27. <https://doi.org/10.1183/2312508x.10020617>.
2. World Health Organization. *Global Tuberculosis Report*; WHO: Geneva, Switzerland, 2021.
3. World Health Organization. Tuberculosis. 2022. Available online: https://www.who.int/health-topics/tuberculosis#tab=tab_1 (accessed on 17 February 2022).
4. Nakajima, H. Tuberculosis: A global emergency. *World Health* **1993**, *46*, 3.
5. Bruchfeld, J.; Correia-Neves, M.; Källénus, G. Tuberculosis and HIV Coinfection: Table 1. *Cold Spring Harb. Perspect. Med.* **2015**, *5*, a017871. <https://doi.org/10.1101/cshperspect.a017871>.
6. Shyam, M.; Shilkar, D.; Verma, H.; Dev, A.; Sinha, B.N.; Brucoli, F.; Bhakta, S.; Jayaprakash, V. The Mycobactin Biosynthesis Pathway: A Prospective Therapeutic Target in the Battle against Tuberculosis. *J. Med. Chem.* **2020**, *64*, 71–100. <https://doi.org/10.1021/acs.jmedchem.0c01176>.
7. Stirrett, K.L.; Ferreras, J.; Jayaprakash, V.; Sinha, B.N.; Ren, T.; Quadri, L.E. Small molecules with structural similarities to siderophores as novel antimicrobials against Mycobacterium tuberculosis and Yersinia pestis. *Bioorg. Med. Chem. Lett.* **2008**, *18*, 2662–2668. <https://doi.org/10.1016/j.bmcl.2008.03.025>.
8. Ferreras, J.A.; Gupta, A.; Amin, N.D.; Basu, A.; Sinha, B.N.; Worgall, S.; Jayaprakash, V.; Quadri, L.E.N. Chemical scaffolds with structural similarities to siderophores of non-ribosomal peptide–polyketide origin as novel antimicrobials against Mycobacterium tuberculosis and Yersinia pestis. *Bioorg. Med. Chem. Lett.* **2011**, *21*, 6533–6537.
9. Shyam, M.; Verma, H.; Bhattacharje, G.; Mukherjee, P.; Singh, S.; Kamilya, S.; Jalani, P.; Das, S.; Dasgupta, A.; Mondal, A.; et al. Mycobactin Analogues with Excellent Pharmacokinetic Profile Demonstrate Potent Antitubercular Specific Activity and Exceptional Efflux Pump Inhibition. *J. Med. Chem.* **2022**, *65*, 234–256. <https://doi.org/10.1021/acs.jmedchem.1c01349>.
10. Dassault Systèmes. *BIOVIA Discovery Studio Visualizer*; V16.1.0.15350. Dassault Systèmes: 2016.
11. Pettersen, E.F.; Goddard, T.D.; Huang, C.C.; Couch, G.S.; Greenblatt, D.M.; Meng, E.C.; Ferrin, T.E. UCSF Chimera—a visualization system for exploratory research and analysis. *J. Comput. Chem.* **2004**, *25*, 1605–1612. <https://doi.org/10.1002/jcc.20084>.
12. Bjelkmar, P.; Larsson, P.; Cuendet, M.A.; Hess, B.; Lindahl, E. Implementation of the CHARMM Force Field in GROMACS: Analysis of Protein Stability Effects from Correction Maps, Virtual Interaction Sites, and Water Models. *J. Chem. Theory Comput.* **2010**, *6*, 459–466. <https://doi.org/10.1021/ct900549r>.
13. Abraham, M.J.; Murtola, T.; Schulz, R.; Páll, S.; Smith, J.C.; Hess, B.; Lindahl, E. GROMACS: High performance molecular simulations through multi-level parallelism from laptops to supercomputers. *SoftwareX* **2015**, *1*–2, 19–25. <https://doi.org/10.1016/j.softx.2015.06.001>.
14. Varadi, M.; Anyango, S.; Deshpande, M.; Nair, S.; Natassia, C.; Yordanova, G.; Yuan, D.; Stroe, O.; Wood, G.; Laydon, A.; et al. AlphaFold Protein Structure Database: Massively expanding the structural coverage of protein-sequence space with high-

- accuracy models. *Nucleic Acids Res.* **2022**, *50*, D439–D444. <https://doi.org/10.1093/nar/gkab1061>. PMID: 34791371; PMCID: PMC8728224.
15. Berman, H.M.; Westbrook, J.; Feng, Z.; Gilliland, G.; Bhat, T.N.; Weissig, H.; Shindyalov, I.N.; Bourne, P.E. The Protein Data Bank. *Nucleic Acids Res.* **2000**, *28*, 235–242. <https://doi.org/10.1093/nar/28.1.235>.
 16. Rizvi, S.M.D.; Shakil, S.; Haneef, M. A simple click by click protocol to perform docking: Autodock 4.2 made easy for non-bioinformaticians. *EXCLI J.* **2013**, *12*, 830–857.
 17. Daina, A.; Michielin, O.; Zoete, V. SwissADME: A free web tool to evaluate pharmacokinetics, drug-likeness and medicinal chemistry friendliness of small molecules. *Sci. Rep.* **2017**, *7*, 1–13.
 18. Pires, D.E.V.; Blundell, T.L.; Ascher, D.B. pkCSM: Predicting Small-Molecule Pharmacokinetic and Toxicity Properties Using Graph-Based Signatures. *J. Med. Chem.* **2015**, *58*, 4066–4072. <https://doi.org/10.1021/acs.jmedchem.5b00104>.
 19. Pronk, S.; Páll, S.; Schulz, R.; Larsson, P.; Bjelkmar, P.; Apostolov, R.; Shirts, M.R.; Smith, J.C.; Kasson, P.M.; Van Der Spoel, D.; et al. GROMACS 4.5: A high-throughput and highly parallel open source molecular simulation toolkit. *Bioinformatics* **2013**, *29*, 845–854. <https://doi.org/10.1093/bioinformatics/btt055>.
 20. Zoete, V.; Cuendet, M.A.; Grosdidier, A.; Michielin, O. SwissParam: A fast force field generation tool for small organic molecules. *J. Comput. Chem.* **2011**, *32*, 2359–2368.